**Supplementary Information**

# Ultrasonic-assisted Europium Decorated Cuprous Oxide Nanoparticles: Exploring their Photothermal Capabilities and Antioxidant Properties for Biomedical Applications

Sarmistha Mazumder[a] , Tiasa Das[c] and *Raviraj Vankayala[a,b,c]

[a]*Joint Center for Medical Technologies, Indian Institute of Technology, Jodhpur 342030, Rajasthan, India.*

[b]*Department of Interdisciplinary Research Division Smart Healthcare, Indian Institute of Technology, Jodhpur 342030, Rajasthan, India.*

[c]*Department of Bioscience & Bioengineering, Indian Institute of Technology, Jodhpur 342030, Rajasthan, India.* *E-mail: rvankayala@iitj.ac.in

## Estimation of Photothermal Conversion Efficiency

The photothermal conversion efficiencies of the Eu-$Cu_2O$ NPs and $Cu_2O$ NPs were determined according to previously reported methods. Detailed calculation is as follows.

$$\eta = \frac{hs\,(T_{max} - T_0) - Q_{Dis}}{I\left(1 - 10^{-A_{808}}\right)} \qquad \ldots. (1)$$

*h* is the heat transfer coefficient; *S* is the surface area of the container; the value of *hS* is obtained from Eq. 4 and Fig. 4d and 4f.

The maximum steady temperature ($T_{max}$) of the solution of Eu-$Cu_2O$ NPs and $Cu_2O$ NPs was 55.3 ° C and 46.6 ° C respectively.

The ambient temperature ($T_o$) of the solution of Eu-$Cu_2O$ NPs and $Cu_2O$ NPs was 28.4 ° C and 24 ° C, respectively.

Therefore, the temperature change ($T_{max} - T_0$) of the solution of Eu-$Cu_2O$ NPs and $Cu_2O$ NPs was 26.9 ° C and 22.6 ° C, respectively.

The laser power *I* is 1W. The absorbances of Eu-$Cu_2O$ NPs and $Cu_2O$ NPs at 808 nm $A_{808}$ were 0.282 and 0.228, respectively. $Q_{Dis}$ denotes the heat dissipated from the light absorbed by the solvent and container.

To calculate *hS,* a dimensionless parameter θ was introduced as follows:

$$\theta = \frac{T - T_0}{T_{max} - T_0} \qquad \ldots. (2)$$

A sample system time constant $t_s$ was calculated as Eq. 3

$$t = - t_s \ln(\theta) \qquad \ldots.. (3)$$

According to figures 4d and 4f, $t_s$ was calculated to be 489.67 s and 591.161 s for Eu-$Cu_2O$ NPs and $Cu_2O$ NPS, respectively.

$$hS = \frac{m_D C_D}{\tau_s} \qquad \text{…….. (4)}$$

Additionally, *m* is 1g, and *C* is 4.2 J/g ° C. Based on Eq . 4, *hS* is measured to be 8.5 mW/ °C and 7.1 mW/ °C for Eu-$Cu_2O$ NPs and $Cu_2O$ NPs respectively.

$Q_{Dis}$ measured heat dissipated from the light absorbed by the quartz sample cell that was measured using a quartz cuvette containing pure water and found to be 2.1 W

Substituting the values of all parameters in Eq. 1, the photothermal conversion efficiency (η) at 808 nm of Eu-$Cu_2O$ NPs and $Cu_2O$ NPs was calculated to be 44 % and 36 %.

**Estimation of Crystallite Size**

Estimation of Crystallite size from XRD data using the Scherrer equation, given by:

$D = (K.\lambda)/(\beta\ cos\theta\ )$ …… (5)

D=crystallite size (nm), K = Shape factor (0.9 for spherical nanoparticles) $\lambda$: for Cu K-alpha, 0.15418 nm), $\beta$: Full Width at Half Maximum (FWHM) of the peak (in radians).

For Eu-$Cu_2O$ NPs, FHWM = 0.57203° = .00998 radians
For $Cu_2O$ NPs, FHWM = 0.38207° = .00667 radians

$\theta$: Bragg angle (in radians), $2\theta$= 26.4°, $\theta$=.2304 radians

For Eu-$Cu_2O$ NPs, D= (0.9) (0.15418)/ (0.00998) cos (.2304) = 14.28 nm

For $Cu_2O$ NPs, D= (0.9) (0.15418)/ (0.00667) cos (.2304) = 21.37 nm

| Entry | Mean particle diameter | PDI | Zeta Potential |
|---|---|---|---|
| $Cu_2O$ NPs | 236.67± 1.52 nm | 0.135 | -22.1± 0.12 mV |
| Eu-$Cu_2O$ NPs (.1%) | 219.67±2.08 nm | 0.153 | 1.4 ± 0.20 mV |
| Eu-$Cu_2O$ NPs (.25%) | 229.33±17.89 nm | 0.291 | 17.8 ± 0.38 mV |
| Eu-$Cu_2O$ NPs (.5%) | 166.67 ± 2.52 nm | 0.136 | -22.7 ± 0.55 mV |

**Table S1.** Table representing the mean particle diameters, PDI and zeta-potential values measured using DLS for various nanoparticles.

| Entry | Cell Line | Test Method | Incubation period | Cell Viability | Ref. |
|---|---|---|---|---|---|
| Cuprous oxide ($Cu_2O$) nanoparticles | B16-F10 (Melanoma) | MTT | 48 h | 50% at 1.992 mg/ml | [37] |
| ZnO@polymer core-shell nanoparticles | U251 (Glioblastoma) | MTT | 48 h | ~80% at 10 mg/ml | [S1] |
| ‘? Dextran-coated $CeO_2$ Nanoparticles | MG-63 (Osteosarcoma) | MTS | 24 h | 50% at >250 mg/ml | [S2] |
| $TiO_2$-DOX nanoparticles | MCF-7/ADM (Breast cancer) | MTT | 24 h | ~84% at 10 mg/ml DOX | [S3] |
| Iron doped Copper oxide nanoparticles | C6 (Glioma) | LDH | 5 h | ~45% at 1000 mM | [16] |
| Europium-doped $CeO_2$ nanoparticles | BV2 (Glial Cells) | MTT | 4 h | 60% at 1 mg/ml | [45] |
| Europium decorated $Cu_2O$ nanoparticles | KB (Epidermal Carcinoma) | PI cell death assay using flow cytometry | 4 h | ~80% at 50 mg/ml | Present work |

**Table S2.** Comparative analysis of cellular viabilities of different metal oxide nanoparticles.

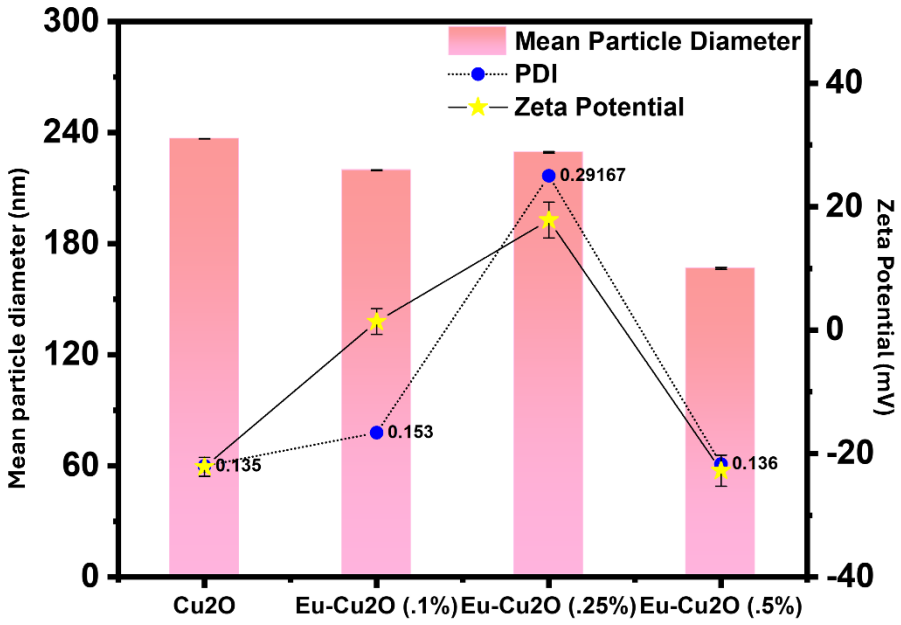


**Fig. S1.** DLS analysis of undecorated $Cu_2O$ NPs and decorated Eu-$Cu_2O$ NPs with variable europium content.

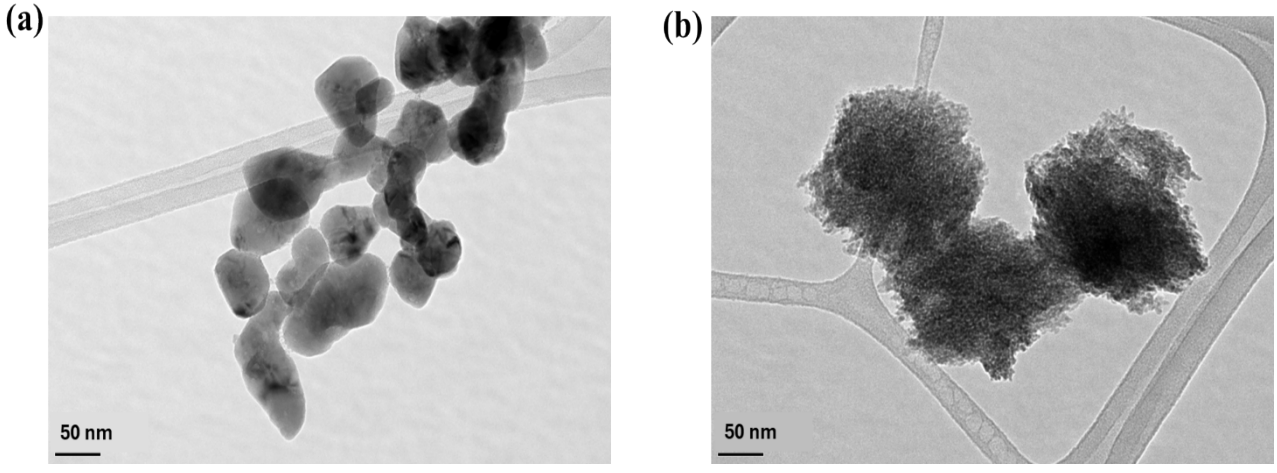


**Fig. S2.** TEM images of (a) $Cu_2O$ NPs and (b) Eu-$Cu_2O$ NPs.

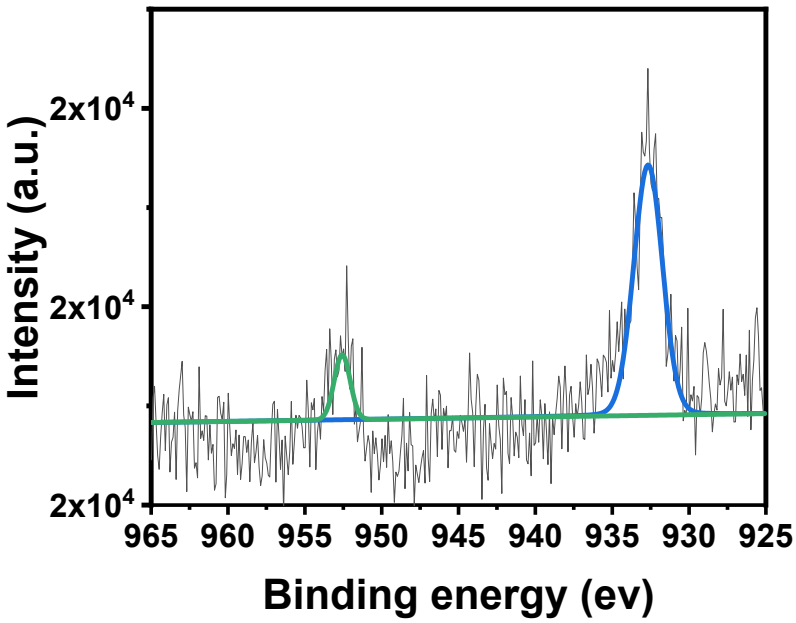


**Fig. S3.** XPS Elemental spectrum (Cu 2p) of pristine $Cu_2O$ NPs

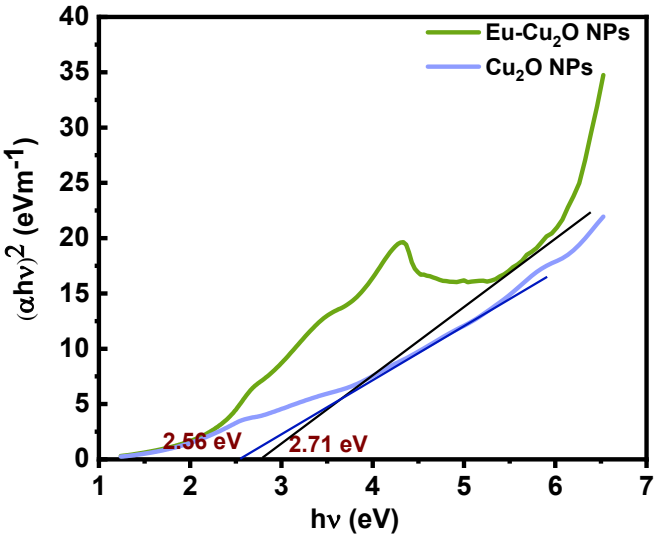


**Fig. S4.** Tauc Plot for direct band gap energy analysis of Eu-$Cu_2O$ NPs and $Cu_2O$ NPs.

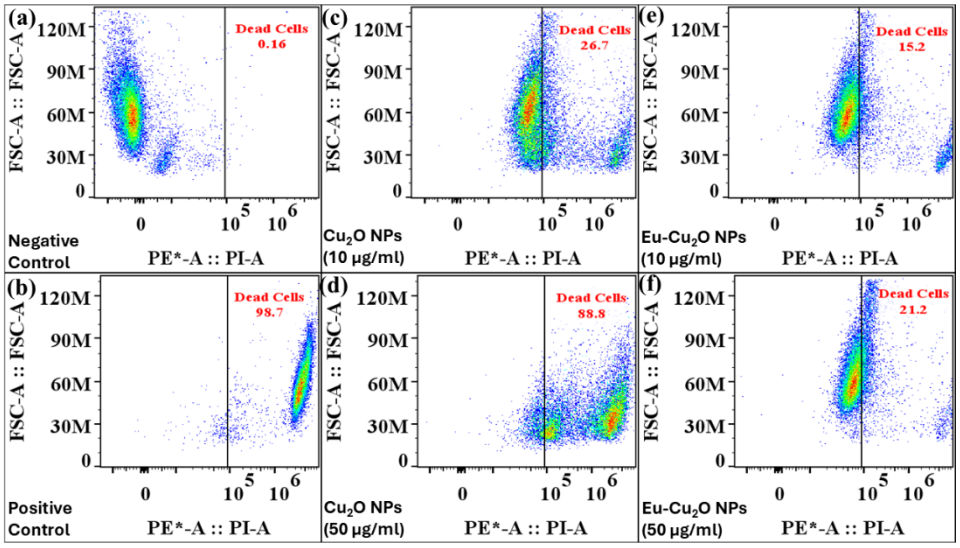


**Fig. S5.** Cell viability assay (dark) using flow cytometry with propidium iodide staining. (a) Untreated cells (b) induced dead cells (c) Cells treated with $Cu_2O$ NPs (10 µg/mL) (d) Cells treated with $Cu_2O$ NPs (50 µg/mL) (e) Cells treated with Eu-$Cu_2O$ NPs (10 µg/mL) (f) Cells treated with Eu-$Cu_2O$ NPs (50 µg/mL).

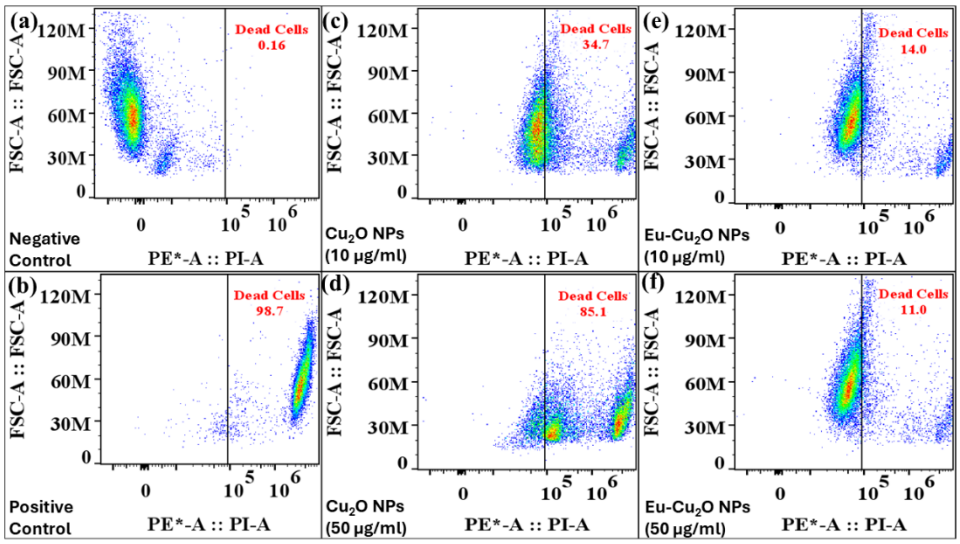


**Fig. S6.** Cell viability assay (under NIR irradiation) using flow cytometry with propidium iodide staining. (a) Untreated cells (b) induced dead cells (c) Cells treated with $Cu_2O$ NPs (10 µg/mL) (d) Cells treated with $Cu_2O$ NPs (50 µg/mL) (e) Cells treated with Eu-$Cu_2O$ NPs (10 µg/mL) (f) Cells treated with Eu-$Cu_2O$ NPs (50 µg/mL).

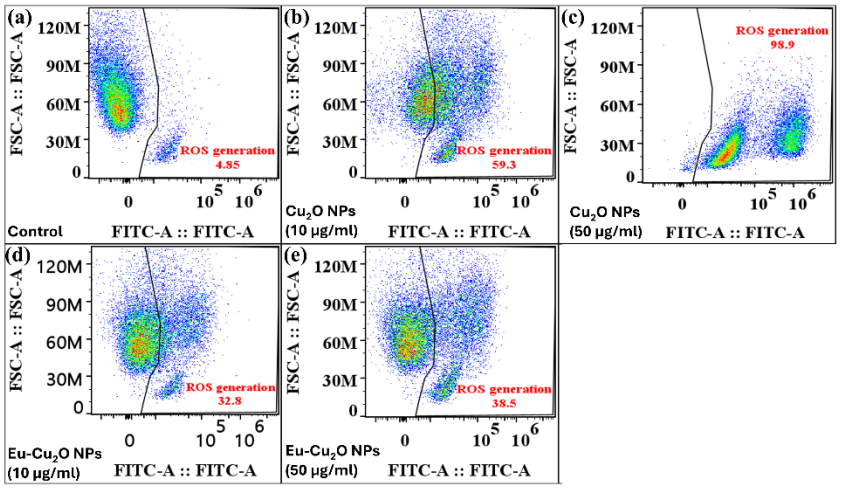


**Fig. S7.** DCFH-DA assay (dark) for ROS detection using flow cytometry in (a) Untreated cells (b) Cells treated with $Cu_2O$ NPs (10 µg/mL) (c) Cells treated with $Cu_2O$ NPs (50 µg/mL) (d) Cells treated with Eu-$Cu_2O$ NPs (10 µg/mL) (e) Cells treated with Eu-$Cu_2O$ NPs (50 µg/mL)

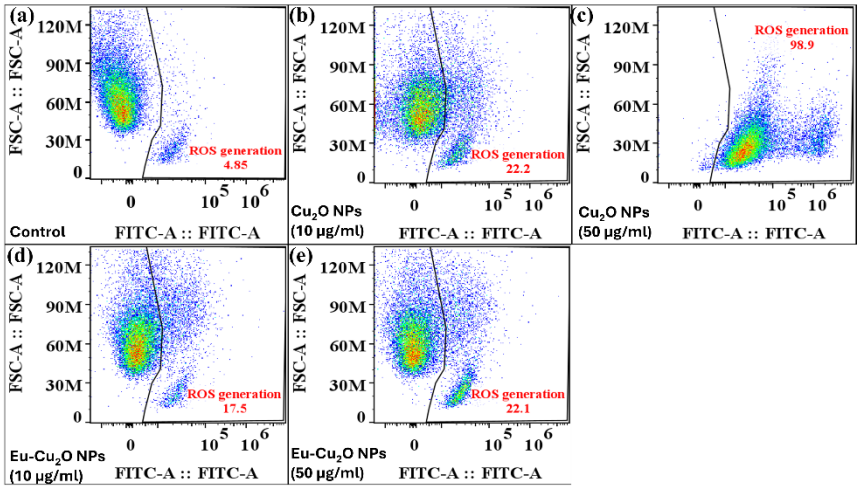


**Fig. S8.** DCFH-DA assay (NIR irradiated) for ROS detection using flow cytometry in (a) Untreated cells (b) Cells treated with $Cu_2O$ NPs (10 µg/mL) (c) Cells treated with $Cu_2O$ NPs (50 µg/mL) (d) Cells treated with Eu-$Cu_2O$ NPs (10 µg/mL) (e) Cells treated with Eu-$Cu_2O$ NPs (50 µg/ml)

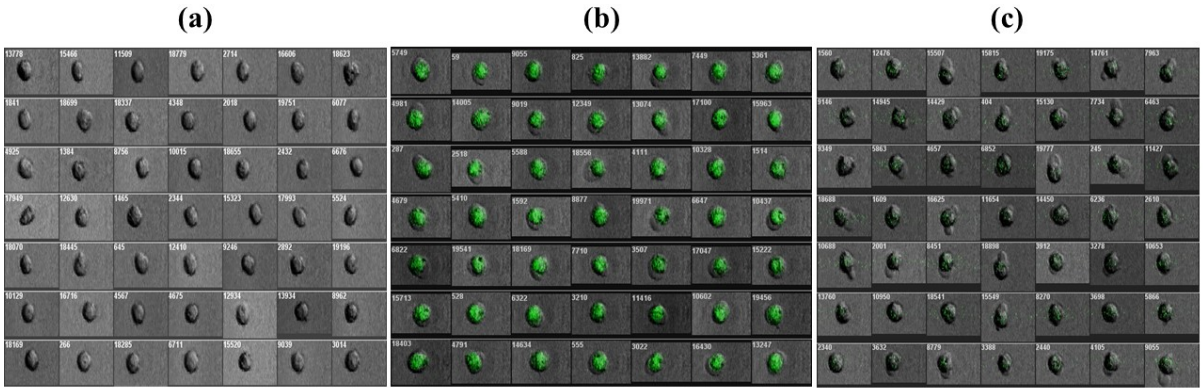


**Fig. S9.** Representative images of cells as obtained from Image enabled Flow Cytometry (BD FACS Discover S8) for (a) untreated (b) $Cu_2O$ NPs (50 µg/mL) and (c) Eu-$Cu_2O$ NPs (50 µg/mL) treated cells for estimation of ROS generation on light irradiation using DCFH-DA Assay. Green fluorescence indicates total ROS generation. The images have been processed

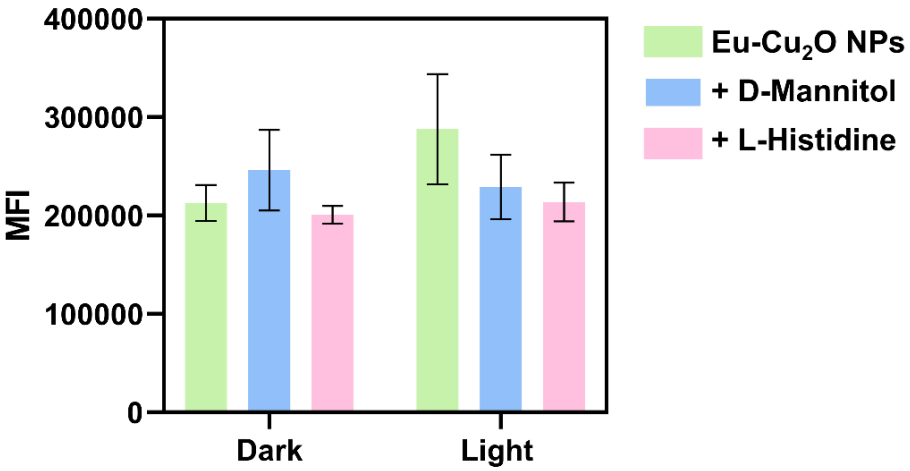


using BD CellView.

**Fig. S10.** ROS quenching studies to study ROS generation by Eu-$Cu_2O$ NPs through the flow cytometric approach, using DCFH-DA as the fluorescent probe and ROS quenchers (D-mannitol and L-histidine). (n=3)

**Supplementary References:**

[S1] Z.Y Zhang, Y. D. Xu, Y. Y Ma, L. L Qiu, Y. Wang, J. L. Kong, H.M Xiong, *Angew. Chem*., 2013, **52(15)**,4127-4131.

[S2] E. Alpaslan, H. Yazici, N. H. Golshan, K. S. Ziemer and T. J. Webster, 2015, *ACS Biomater Sci Eng*, **1**, 1096–1103.

[S3] W Ren, L Zeng, Z Shen, L Xiang, A Gong, J Zhang, C Mao, A Li, T Paunesku, G E. Woloschak, N S. Hosmaned, A Wu, 2013, *RSC Adv*., **3**, 20855.